

TURBULENCE-INDUCED SECONDARY FLOWS IN A SQUARE DUCT USING A MULTIPLE-RELAXATION-TIME LATTICE-BOLTZMANN APPROACH

Martin J. Pattison
MetaHeuristics LLC,
209 W. Alamar Ave., Suite A
Santa Barbara, CA 93105, USA
martin@metah.com

Kannan N. Premnath and Sanjoy Banerjee
Department of Chemical Engineering,
University of California,
Santa Barbara, CA 93106, USA
nandha@metah.com, sanjoy@engineering.ucsb.edu

ABSTRACT

Turbulent fluid flow through a square duct is characterised by the existence of net flows in directions perpendicular to the duct axis. These secondary circulations take the form of eight counter-rotating vortices, bounded by the wall, a wall bisector and a corner bisector. The velocities are relatively small, significantly lower than the turbulent fluctuations, and are relatively difficult to capture in numerical simulations. A multiple-relaxation-time lattice Boltzmann method has been applied to this problem, using a Smagorinsky eddy viscosity subgrid scale model with a van Driest wall damping function to model the unresolved stresses. A Reynolds number of 300 (based on mean friction velocity and duct width) was used and the flow was driven by a pressure gradient in the streamwise direction, with periodic boundary conditions applied in this direction. The large eddy simulations using this method correctly predicted the existence of the secondary flows, and turbulent statistics were found to be in good quantitative agreement with prior data from high resolution numerical simulations.

INTRODUCTION

A classic example of Prandtl's *secondary flows of the second kind* is presented by turbulent fluid flow through a square duct, in which circulations in directions perpendicular to the bulk flow are found. These secondary flows also arise in turbulent flow through channels of other non-circular cross-sections, but are not found in laminar flows. Although long recognised to be associated with turbulence, the exact cause of these circulations has been a subject of debate, though it is generally recognized to be associated with the inhomogeneity and anisotropy in the Reynolds stress in the cross-sectional plane.

In a square duct, the time-averaged velocity fields reveal these secondary flows as a set of eight vortices, each one enclosed by a wall, a corner bisector and a wall bisector. The general features are not sensitive to the Reynolds number, except that it should be high enough that the flow be fully turbulent. The velocities associated with these flows is relatively small, of the order of 1% of the mean streamwise velocity, and thus significantly smaller than the turbulent velocity fluctuations. The mechanisms responsible for the secondary flows result from a fine balance involving the gradients in the Reynolds stress and pressure strain

terms, making the square duct a particularly challenging problem for turbulence models. For example, computations based on commonly used Reynolds-averaged models, such as the $k-\epsilon$ model, do not perform well, while more complex anisotropic Reynolds stress models have been successful to a degree, though not without *a priori* information on the stress terms. In this regard, eddy capturing schemes based on subgrid scale models appears to be more promising.

In this work, the lattice Boltzmann method (LBM) is applied to the turbulent duct flow problem. The LBM is an approach based on kinetic theory, in which kinetic equations are solved for a set of distribution functions, from which the macroscopic variables (velocity, pressure) can be recovered. This is somewhat different from other approaches in which finite difference or spectral methods are used to directly solve the equations governing the flow of fluids. The approach taken uses the multiple-relaxation-time (MRT) model, a recent formulation developed by d'Humières et al. (2002) and subsequently extended by Premnath and Abraham (2007). This model offers better stability and accuracy than earlier models based on the Bhatnagar-Gross-Krook (BGK, 1954) approximation and using just a single relaxation time (SRT).

With the LBM being a comparatively recent approach to computational fluid dynamics, relatively little work has been done to assess its suitability for turbulent flows, most work having focused on laminar flow at low Reynolds numbers. However, recent studies using the MRT model (e.g. Yu et al., 2006) have demonstrated much better performance than with the earlier SRT model, which is likely to increase interest in the application of the LBM to turbulent flows.

The MRT-LBM has not yet been thoroughly assessed for wall-bounded turbulent flows, and the principal objective of this work was to use the turbulent duct flow problem to determine how well the LBM would perform for bounded flows. A subgrid scale model was used, and the unresolved turbulence scales were dealt with by using a Smagorinsky eddy viscosity model, with a van Driest damping function applied near to the walls, so as to perform large eddy simulations (LES). As previously mentioned turbulent duct flow is a challenging case and Reynolds averaged turbulence models generally cannot predict the secondary flows adequately. For this reason it is employed as the benchmark problem in this work.

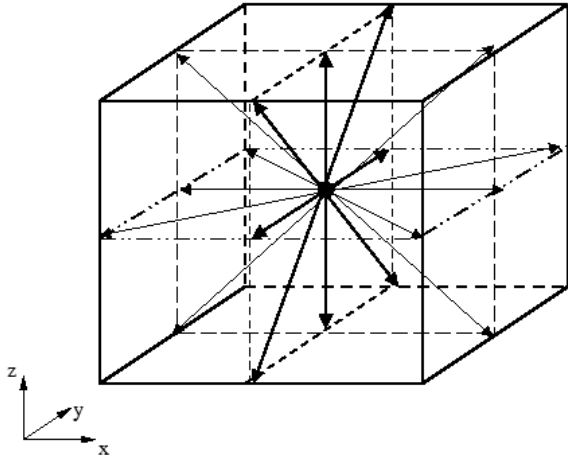


Figure 1: Schematic illustration of the 19-velocity model.

SOLUTION PROCEDURE

Lattice Boltzmann method

The lattice Boltzmann method (LBM) is a relatively recent approach for solving fluid mechanics problems (Chen and Doolen, 1998; Succi, 2001). It is based on the solution of a kinetic equation, the lattice Boltzmann equation (LBE), which describes the evolution of distributions of particles on a lattice whose collective behavior reproduces fluid flow. The lattice, possessing sufficient symmetry, restricts the collisions and movements of particle populations along discrete directions in such a way that in the continuum, fluid flow represented by weakly compressible Navier-Stokes equations is reproduced. The attractiveness of the LBM comes from the simplicity of the numerical procedure, avoiding the use of time consuming Poisson-type equation for pressure field, and ease in handling boundary conditions for representation of complex geometries. Moreover, LBM involves algorithms that are local and explicit, resulting in excellent performance on a variety of parallel computers with near-linear scaling and thus suitable for large problems.

The LBE is discretised and solved on a grid, and in three dimensions a cubic grid is used, and 15- or 19- discrete velocity models are commonly used, though models with 18 or 27 velocities are also found occasionally. In this work, a 19-velocity model was used, due to its superior numerical stability, and this is shown in Fig. 1.

The distribution function f_α is calculated using a two step procedure comprising a so-called collision step and a streaming step. In the MRT formulation, the following kinetic equations are used (d’Humières et al., 2002; Premnath and Abraham, 2007):

$$\begin{aligned} \tilde{f}_\alpha(\mathbf{x}, t) &= - \sum_{\beta} \Lambda_{\alpha\beta} (f_\beta - f_\beta^{eq}) \\ &+ \sum_{\beta} \left(\mathbf{I}_{\alpha\beta} - \frac{1}{2} \Lambda_{\alpha\beta} \right) S_\beta \delta t \end{aligned} \quad (1-a)$$

$$f_\alpha(\mathbf{x} + \mathbf{e}_\alpha \delta t, t + \delta t) = \tilde{f}_\alpha(\mathbf{x}, t) \quad (1-b)$$

The first term on the right hand side (RHS) of Eq. (1-a) represents the cumulative effect of particle collisions on the evolution of the distribution function f_α , and can be thought of as representing the effects of viscosity, as well as other

processes; the subscripts α and β represent the discrete velocity vectors. Collision is considered as a relaxation process in which f_β relaxes to its local equilibrium value f_β^{eq} at a rate determined by the relaxation time matrix $\Lambda_{\alpha\beta}$. The MRT model has a generalised collision matrix with multiple relaxation times corresponding to the underlying physics: the macroscopic fields such as densities, momentum and stress tensors are given as various kinetic moments of the distribution function. For example, collision does not alter the densities ρ and momentum $\rho \mathbf{u}$, while the stress tensors relax during collisions at rates determined by fluid properties such as the shear and bulk viscosities. Thus certain relaxation times forming components of the collision matrix $\Lambda_{\alpha\beta}$ in the MRT model are developed to reflect the underlying physics, while those which do not affect hydrodynamics are chosen to enhance the numerical stability of the approach. For more details, the reader is referred to d’Humières et al. (2002) and Premnath and Abraham (2007).

The second term on the RHS of Eq. (1-a) introduces changes in the evolution of distribution function from driving forces \mathbf{F} , such as gravity or an imposed pressure gradient used to drive the flow, through a source term S_α ; the tensor $\mathbf{I}_{\alpha\beta}$ is the identity matrix.

At this point is worth noting that the commonly used SRT model uses a scalar relaxation parameter in place of the tensors $\Lambda_{\alpha\beta}$ and there is no summation for the terms on the right. Also note that the implementation of Eq. (1-a) does not involve direct summation as shown, but uses a highly optimised procedure that involves transformations into moment space and exploits certain properties of $\Lambda_{\alpha\beta}$ (d’Humières et al., 2002; Premnath and Abraham, 2007; Premnath et al., 2007). With these optimisations, it is found that despite its much greater complexity, the MRT only takes about 10–30% more CPU time than the BGK model. Thus Eq. (1-a) provides the post-collision value of the distribution function given by \tilde{f}_α .

Equation (1-b) is known as the advection, or streaming, step and deals with the change in the distribution function during a time interval δt , as the particles propagate from location \mathbf{x} to their adjacent location $\mathbf{x} + \mathbf{e}_\alpha \delta t$, with a velocity \mathbf{e}_α along the characteristic direction α .

The local macroscopic density and velocity fields are then given by taking appropriate kinetic moments as

$$\rho = \sum_{\alpha=0}^{18} f_\alpha \quad (2)$$

$$\rho \mathbf{u} = \sum_{\alpha=0}^{18} f_\alpha \mathbf{e}_\alpha + \frac{1}{2} \mathbf{F} \delta t \quad (3)$$

and the pressure field p may be written as

$$p = c_s^2 \rho \quad (4)$$

where $c_s = \delta_x / (\delta t \sqrt{3})$ is the speed of sound.

The behaviour of the populations represented by the distribution function \mathbf{f} corresponds to that of fluid flow, and the incompressible Navier–Stokes equations can be recovered from the lattice Boltzmann equations for the case of low Mach number ($v \ll c_s$). The discussion of the MRT model presented here has been relatively brief, but more detailed descriptions can be found in the aforementioned papers.

Two important points to note are that there is no pressure Poisson equation to solve, and that the solution scheme is explicit, with information required from neighbouring

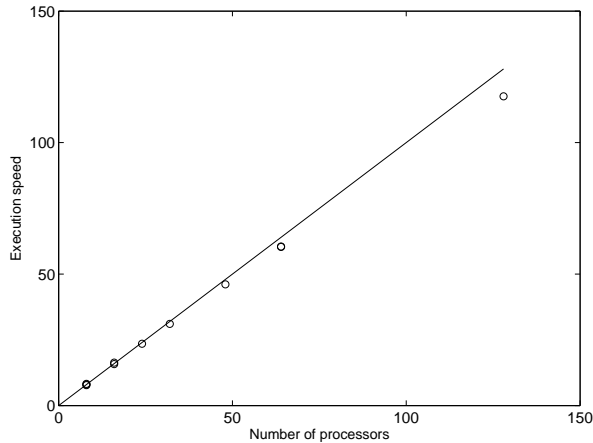


Figure 2: Parallel performance of the lattice Boltzmann code for turbulent flow with a grid of $2400 \times 120 \times 120$. Circles are data points and line is speed for linear scaling. Speeds are normalised by one eighth of the speed using eight processors.

nodes only. The solution of the Poisson equation is time consuming and typically takes 80–90% of the CPU time in traditional CFD solvers (Madabhushi and Vanka, 1991; Premnath et al., 2002); its absence means that LBM codes are relatively fast on a per time step per grid point basis. The explicit nature of the computations means that codes based on the LBM can run very efficiently on parallel architectures, and this is one of the main motivations for its use.

As an example, Fig. 2 shows the results of some parallel performance tests using our lattice Boltzmann code. The case simulated was turbulent flow through a cylindrical pipe using a Smagorinsky turbulence model modulated by a wall damping function. A grid size of $2400 \times 120 \times 120$ was used and data were obtained by recording the time taken to perform a fixed number (about 200) of time steps. The code was run on between 8 and 128 processors on the US Department of Energy’s supercomputer BASSI and the speeds shown in the plot are normalised such that the mean speed on one 8 processor node is eight. For the 128 processor case, the computational speed was 14.7 times that with 8 processors, which corresponds to 92% of that which would be obtained with linear scaling. It was found that for the tests involving just one node, the times taken varied significantly, by up to 6%, though when using many nodes the run times were more or less constant. This suggests that about 3% of the fall off in performance could be accounted for by variations in the speed of the different nodes. Similar performance figures have been found for flows with magnetohydrodynamic effects (Pattison et al, 2007).

Turbulence model

The standard Smagorinsky model has been implemented to account for the effect of unresolved scales in large eddy simulations (LES). In this model, the eddy viscosity, ν_t , is calculated from

$$\nu_t = (C_s \Delta)^2 \bar{S}, \quad \bar{S} = \sqrt{2S_{ij}S_{ij}} \quad (5)$$

where C_s is a constant and Δ is a length scale. In the present study, the length scale was taken to be equal to the grid spacing, and C_s was set to 0.12. The strain rate tensor is given by $S_{ij} = 1/2(\partial_j u_i + \partial_i u_j)$ and was calculated di-

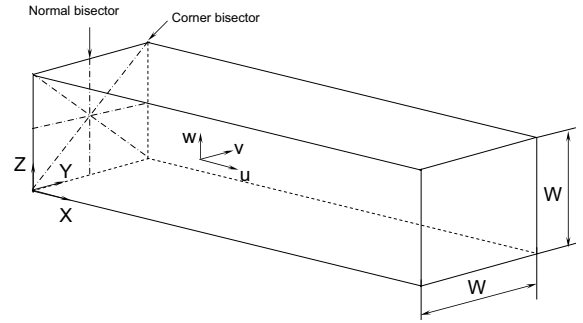


Figure 3: Schematic diagram showing geometry modelled.

rectly from the non-equilibrium part of the moments – this is computationally more efficient than using finite differences, and simplifies the calculation for complex geometries.

To account for the effect of walls on the turbulence, the length scale was modified using the van Driest damping function (1956)

$$\Delta = \delta_x [1 - \exp(-y^+/A^+)] \quad (6)$$

where $y^+ = yu_*/\nu_0$ is the normalised distance from the the wall, u_* is the friction velocity and the constant $A^+ = 26$.

SIMULATIONS

A schematic representation of the geometry used is shown in Fig. 3. The shear Reynolds number used was 300. This is defined as $Re_* = u_* w / \nu$ where w is the duct width and the mean friction velocity is calculated from the imposed pressure gradient as $\rho u_*^2 = w |dP/dx|/4$. The dimensionless viscosity (normalised by the grid spacing and time step) was set to 0.001, and a grid size of $432 \times 74 \times 74$ was used.

Periodic boundary conditions were applied in the x (streamwise) direction, and no-slip conditions in the other two directions. The use of grid points within the wall meant that the boundary was half a grid spacing from the outermost points, thus the effective width was 72 grid separations. A uniform grid was used for the simulation, though it should be noted that stretched grids can be used with the LBM for certain problems (He et al., 1996; Premnath and Abraham, 2004). The choice of domain proportions followed the recommendation of Huser and Birigen (1993), who found that a streamwise extent of about six times the duct width was sufficiently long to yield accurate simulations.

For the initial conditions, an approximate velocity field was set up, based on the $1/7$ power law. In order to initiate turbulence, a perturbation profile with sinusoidal fluctuations was superimposed on this, chosen so as to satisfy continuity (Lam, 1989).

The simulation was run using the MRT model (Premnath et al., 2007), with a pressure gradient providing the driving force. A single processor Pentium IV machine was found to be sufficient for this. The computation was run until a statistically steady state was reached, and then continued for a period of over 100 000 time steps over which statistics were collected.

Three main sources of data were used for comparisons with the MRT–LBM simulations. Gavrilakis (1992) performed high resolution DNS at the same Reynolds number as our simulation. Huser and Birigen (1993) also performed DNS of this case, though they used a higher Reynolds number of 600. Comparisons with LES performed by Madabhushi and Vanka (1991), based on a finite difference ap-

proach, are also included to enable the performance of the LBM LES code to be judged against that of another LES code. In addition, experimental data from Cheesewright et al. (1990) for a Reynolds number slightly lower than that in the present simulations was used.

RESULTS

Figure 4 shows contours of the streamwise velocity in the cross-sectional plane. In this plot, the velocity has been averaged over both time and the length of the domain. Figure 5 shows the secondary velocities (the non-streamwise component); in this case, and in all other plots unless otherwise stated, statistics were also averaged over the eight similar octants.

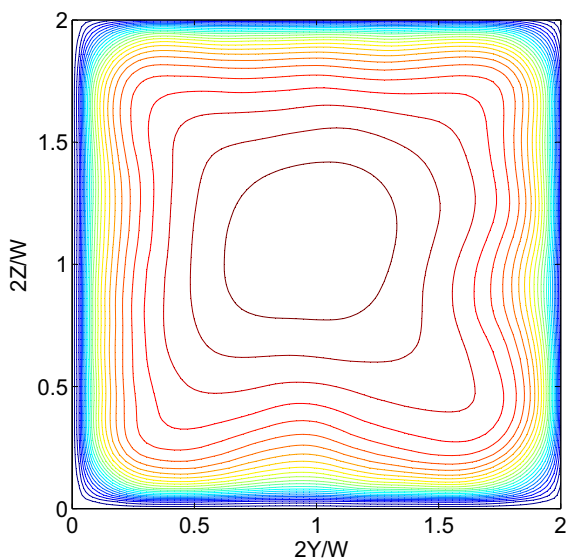


Figure 4: Mean streamwise velocities in the cross-sectional plane.

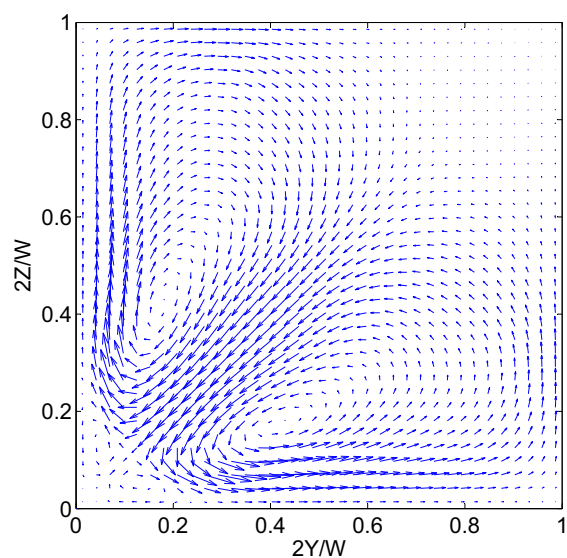


Figure 5: Mean secondary velocity vectors in the cross-sectional plane.

Figure 5 clearly shows the expected vortex moving in a

sense such that fluid moves toward the corner along the corner bisector and away from the wall along the wall bisector. The vortex is centred at about (0.45, 0.18), where the numbers in parentheses are the y and z coordinates normalised with respect to the half width. This compares well with Gavrilakis's DNS which gave the centre at (0.5, 0.2). Madabhushi and Vanka's LES predicted the centre at (0.55, 0.25) and Huser and Birigen's DNS, (at higher Reynolds number) at (0.4, 0.2). The plot also suggests the presence of a small vortex very close to the corner – this was also noticed by Gavrilakis.

The contours of streamwise velocity can be seen to bend toward the walls near to the corners. This is a characteristic of duct flow and is associated with the secondary flow. The secondary vortex transports faster-moving fluid from the central region toward the corners along the corner bisectors while slower-moving fluid from the vicinity of the wall is advected toward the centre near the wall bisectors, resulting in the bulge in the contours.

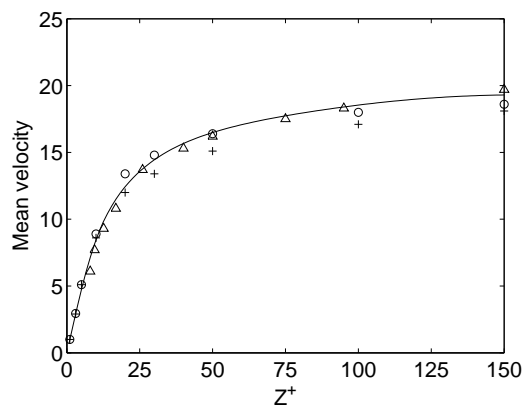


Figure 6: Mean streamwise velocity along wall bisector. Lines are MRT-LBM predictions, circles Huser & Birigen (1993), triangles Madabhushi & Vanka (1991), and crosses Gavrilakis (1992).

Figure 6 shows the mean streamwise velocity along the wall bisector. To be consistent with the data with which it is compared, the velocity is normalised using the local friction velocity at the wall bisector, calculated as $u_{\tau}^2 = \tau/\rho$ where τ is the local wall stress and ρ the density. Distance is plotted in terms of wall units ν/u_{τ} , where ν is the viscosity. When compared with Gavrilakis's DNS (1992), the mean velocity is slightly overpredicted, as is often the case with the lower resolutions used with LES. Huser and Birigen (1993) used a lower resolution in the wall-normal direction than Gavrilakis and this is the likely reason for the higher velocity predicted, though there could also be Reynolds number effects. Also, Huser and Birigen had performed a preliminary DNS at a coarser resolution, and this had given higher velocities than the final DNS.

Turbulence statistics are presented in Fig. 7, which shows the root mean square (rms) velocity fluctuations along a wall bisector, together with data from LES and DNS for comparison. The level of agreement with the DNS data can be seen to be good, and MRT-LBM predictions show significantly better agreement with the DNS data than the other LES, despite the fact that the LBM computations were run with a much coarser resolution in the important near-wall region. The variation in rms velocities is very similar to that found in other wall-bounded flows and comparisons with plane channel data can be found in Gavrilakis's pa-

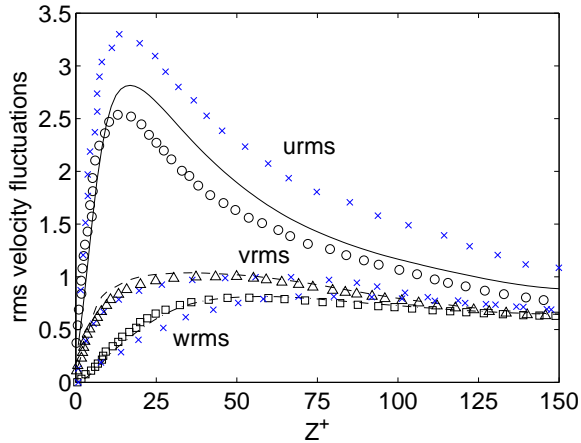


Figure 7: Root mean square velocity fluctuations along wall bisector. Lines are MRT-LBM predictions for $Re_* = 300$, open symbols DNS data of Gavrilakis (1992), and crosses LES data from Madabushi and Vanka (1991). Velocities have been normalised with u_τ .

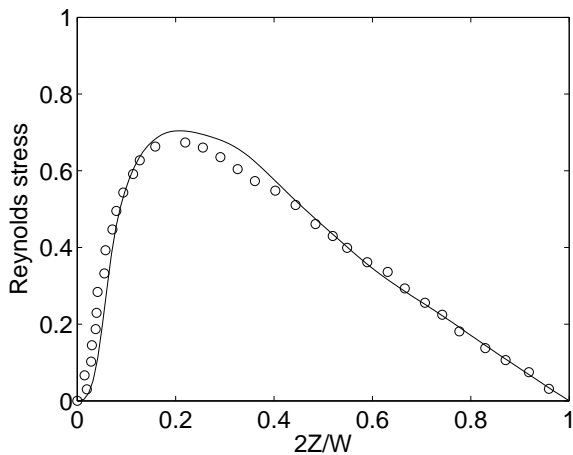


Figure 8: Reynolds stress along wall bisector. Lines are MRT-LBM predictions and circles are DNS data of Gavrilakis (1992).

per. Gavrilakis raised the question of whether the friction velocity at the wall centre, u_τ , or the average friction velocity, u_* , should be used for the normalisation of the data, and noted that agreement with channel data was best if u_τ was used near to the wall and u_* farther out.

The principal component of Reynolds stress $\langle -u'w' \rangle$ along a wall bisector ($y/W = 0.5$) is plotted in Fig. 8. Again, reasonable, though not perfect, agreement with the DNS data can be observed, as is typical of LES. Comparisons with Fig. 7 show that the LBM tends to overpredict the stress where the turbulent intensities are overpredicted and vice versa.

One important assessment of this work was to evaluate the ability of the model to quantitatively capture the secondary circulations. Figure 9 plots the mean spanwise (y -component) velocity profiles along lines of constant y , and compares the predictions with those of Gavrilakis and the experimental data of Cheeswright et al. These plots clearly show quantitative agreement between the different sources.

Figure 10 plots the root mean square fluctuations of the spanwise velocity component. Again comparison with other

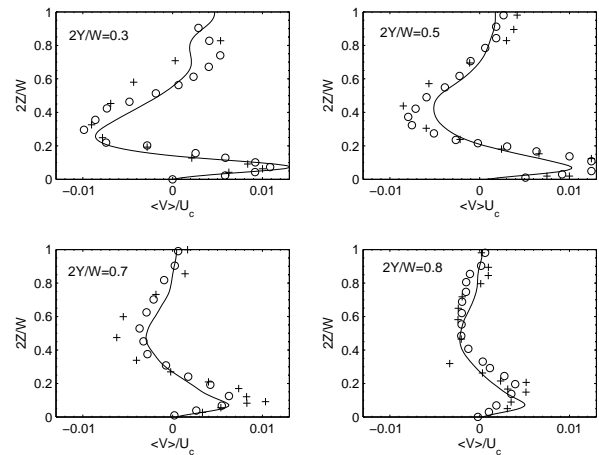


Figure 9: Profiles of mean spanwise velocity. Lines are MRT-LBM, circles DNS (Gavrilakis, 1992) and crosses experimental data (Cheeswright et al., 1990).

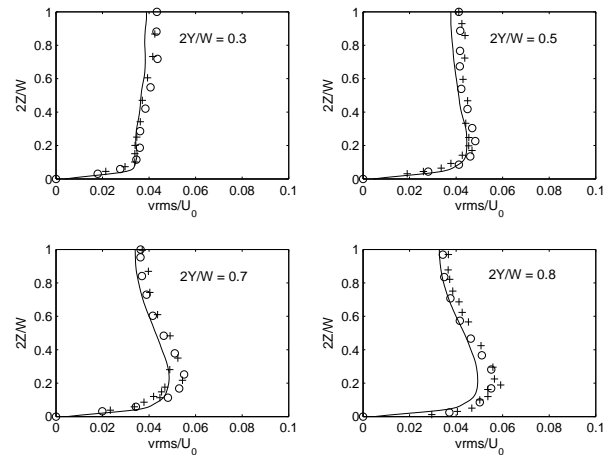


Figure 10: Profiles of rms spanwise velocity. Lines are MRT-LBM, circles DNS (Gavrilakis, 1992) and crosses experimental data (Cheeswright et al., 1990).

data shows close agreement.

CONCLUSIONS

The ability of the MRT-LBM to simulate a wall-bounded turbulent flow in a square duct has been investigated. This case was chosen because it exhibits secondary circulations which are relatively difficult to capture with computational methods; indeed many commonly turbulence fail to reveal these motions. The large eddy simulations were performed with a Smagorinsky model with a wall damping function used for the unresolved stresses.

Analysis of the results showed the four pairs of counter-rotating vortices representing the secondary flows to be present, and comparisons with prior data from Gavrilakis (1992) and Cheeswright et al. (1990) showed the magnitudes of these components to be in good qualitative agreement. Despite the relatively low resolution used (about 4 wall units in the bulk, with 2 wall units next to the wall), the predictions of turbulent fluctuations and streamwise velocities have been within about 10% of the DNS data, and

the LBM showed better agreement than did an earlier finite difference based LES (Madabhushi and Vanka, 1991). When one considers its ability to parallelise, it appears that the LBM shows great potential as a tool for the simulation of complex turbulent flows.

ACKNOWLEDGEMENTS

The development of the lattice Boltzmann code was funded by the US Department of Energy (DOE) under Grant No. DE-FG02-03ER83715 and by NASA under Contract NNL06AA34P. The work used resources of the National Energy Research Scientific Computing Center, which is supported by the Office of Science of DOE under Contract DE-AC03-76SF00098. The authors also acknowledge supercomputing support from the National Center for Supercomputing Applications through Grant No. CTS060027.

REFERENCES

- Bhatnagar, P., Gross, M., and Krook, E., 1954, "A Model for Collision Processes in Gases. I. Small Amplitude Processes in Charged and Neutral One-Component Systems," *Phys. Rev.*, Vol. 94, pp. 511–525.
- Cheesewright, J., McGrath, G., and Petty, D. G., 1990, Aeronautical Engineering Dept. Rep. ER 1101, Queen Mary & Westfield College, London.
- Chen, S. and Doolen, G., 1998, "Lattice Boltzmann Method for Fluid Flows," *Annu. Rev. Fluid Mech.*, Vol. 30, pp. 329–364.
- Gavrilakis, S., 1992, "Numerical Simulation of Low-Reynolds-Number Turbulent Flow through a Straight Square Duct," *J. Fluid Mech.*, Vol. 244, pp. 101–129.
- He, X., Luo, L.-S., and Dembo, M., 1996, "Some Progress in the Lattice Boltzmann Method. Part 1: Non-Uniform Mesh Grids," *J. Comp. Phys.*, Vol. 129, pp. 357–363.
- d'Humières, D., Ginzburg, I., Krafczyk, M., Lallemand, P., and Luo, L.-S., 2002, "Multiple-Relaxation-Time Lattice Boltzmann Models in three Dimensions," *Phil. Trans. R. Soc. Lond. A*, Vol 360, pp. 437–451.
- Huser, A., and Birigen, S., 1993, "Direct Numerical Simulation of Turbulent Flow in a Square Duct," *J. Fluid Mech.*, Vol. 257, pp. 65–95.
- Lam, K., 1989, "Numerical investigation of turbulent flow," PhD Thesis, Univ. California, Santa Barbara.
- Madabhushi, R. K., and S. P. Vanka, 1991, "Large Eddy Simulation of Turbulence Driven Secondary Flow in a Square Duct," *Phys. Fluids A*, Vol. 3, pp. 2734–2745.
- Pattison, M. J., Premnath, K. N., Morley, N. B., and Abdou, M., 2007, "Progress in Lattice Boltzmann Methods for Magnetohydrodynamic Flows Relevant to Fusion Applications," submitted to *Fusion Eng. and Des.*
- Premnath, K. N., and Abraham, J., 2004, "Discrete Lattice BGK Boltzmann Equation Computation of Transient Incompressible Turbulent Jets," *Int. J. Modern Phys. C*, Vol. 15, pp. 699–719.
- Premnath, K. N., Abraham, J., and Magi, V., 2004, "Parallelization of a Multidimensional Code for the Simulation of Flows in Engines: Performance with OpenMP Programming Model," *Proc. High Performance Symp., Advanced Simulation Tech. Conf.*, San Diego, CA.
- Premnath, K.N., and Abraham, J., 2007, "Three-Dimensional Multi-Relaxation-Time Lattice Boltzmann Models for Multiphase Flows," *J. Comp. Phys.*, in press.
- Premnath, K. N., M. J. Pattison and S. Banerjee (2007) "Generalized Lattice Boltzmann Equation with Forcing Term for LES of Bounded Turbulent Flows: Accuracy, Stability and Computational Efficiency," Submitted to *Phys. Rev. E*.
- Succi, S., 2001, "The Lattice Boltzmann Equation for Fluid Dynamics and Beyond," Clarendon Press, Oxford.
- van Driest, E. R., 1956, "On the Turbulent Flow near a Wall," *J. Aerospace Sci.*, Vol 23, pp. 1007-1011.
- Yu, H., Luo, L.-S., and Girimaji, S., 2006, "LES of Turbulent Square Jet Flow using an MRT Lattice Boltzmann Model," *Computers and Fluids*, Vol. 35, pp. 957–965.